Design and synthesis of paramagnetic probes for structural biololgy

Liu, W.

Chapter IV

CLaNP-5 derivatives: An approach to obtain multiple paramagnetic restraints sets from a single mutation site

Abstract

Site-specific labeling *via* disulfide bridges or thioether linkages are widely employed for paramagnetic probe attachment because cysteine residues can be selectively incorporated in protein. In order to investigate protein-protein and protein-ligand interactions, multiple paramagnetic data sets are required; however, finding suitable mutation sites is sometimes difficult, especially for small proteins. An alternative is to attach different paramagnetic probes to same site. Several CLaNP-5 derivatives have been synthesized for this purpose and one of them was tagged to a model protein. The HSQC spectra of methoxyl functionalized CLaNP-5 showed two sets of PCSs. This phenomenon could be explained by an interaction with a neighboring amino acid with the methoxyl group.

Introduction

Lanthanoid complexes have been widely used as paramagnetic centers in high resolution NMR spectroscopy, because the interaction of an unpaired electron provided by lanthanoids with protein nuclei yields significant structural information (Chapter 1). To generate unique paramagnetic effects, lanthanoid probes have to be rigidly and site-specifically attached to proteins. So far, most synthetic probes are tagged to proteins *via* disulfide bonds or thiol alkylation. The advantages of these methods are that the cysteine residues can be selectively incorporated into proteins and these residues react specifically with thiol-reactive groups, avoiding undesired side-products. Multiple unique paramagnetic restraints are required for evaluating protein-protein and protein-ligand interactions. However, finding ideal mutation sites is not easy in many cases, especially for small proteins. Hence, the development of alternative approaches is desirable.

The 12-membered macrocyclic DOTA, an octadentate ligand, is used as a complexing agent, especially for lanthanoid ions. The coordination of DOTA and its analogs to lanthanoid ions is such that two stable enantiomer pairs are formed, namely, capped square antiprism (SA) and twisted capped square antiprism (TSA). These two forms inter-convert slowly on the NMR time scale in solution (Chapter 1). In 2004, pyridine-*N*-oxide was first introduced into DOTA ring and it coordinated to lanthanoid ions *via* a six-membered ring yielding a single conformation, the SA form, in solution.[39,182] Subsequently, two pyridine-*N*-oxides were substituted the opposite acetate arms of a DOTA ring to give *C2*-symmetry forming a powerful paramagnetic NMR probe, **CLaNP-5**. The replacement of pyridine-*N*-oxide with *para*-nitrophenol resulted in a next generation probe, **CLaNP-7**. Both of these probes yielded a single set of PCSs and were used for the study of protein-protein interactions (Chapter 1). They exhibit different magnetic susceptibilities at the same attachment site. Therefore, using different paramagnetic probes at single attachment site could be an alternative approach to obtain multiple data sets.

To demonstrate this idea, several **CLaNP-5** derivatives as well as a model system, the **AMC5-**series, were designed and synthesized (Chart 1). The proton at the para-position of the pyridine-*N*-oxide ring was replaced with different functional groups to modify the magnetic susceptibility of the probes. The ^{1}H NMR spectra of Ln^{3+} **AMC5-**series complexes indicate that only a single enantiomeric pair is present in solution and the magnetic susceptibilities depend on the substituents. However,

two sets PCSs were observed in the HSQC spectrum of **CLaNP-5-OMe** tagged protein and the relative intensity was temperature dependent. Possible explanations and the implications for deriving multiple paramagnetic data sets from a set of related probes are discussed.

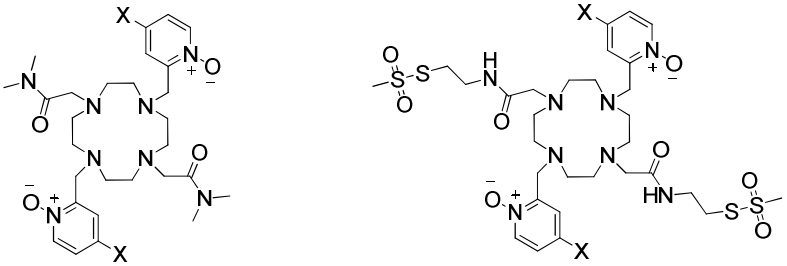

Chart 1. Structures of AMC5 and CLaNP-5 analogs.

Results and discussion

Synthesis of caged lanthanoid NMR probe-5 (CLaNP-5) analogs

The *para*-position in the pyridine-*N*-oxide core is relatively far from the lanthanoid and the substitutions do not have side effect on the overall structure of Ln^{3+} complexes.[39,145] Consequently, the proton could be replaced with different functional groups. The synthesis of **AMC5** is shown in Scheme 1. The commercially available cyclen was converted to selectively protected **1a** and **1b** using a published protocol.[42] The protective groups in **1a** and **1b** were fully removed using TFA and the crude compounds were then reacted with 2-(chloromethyl)pyridine-1-oxide at 80 ^{o}C to obtain **AMC5**.

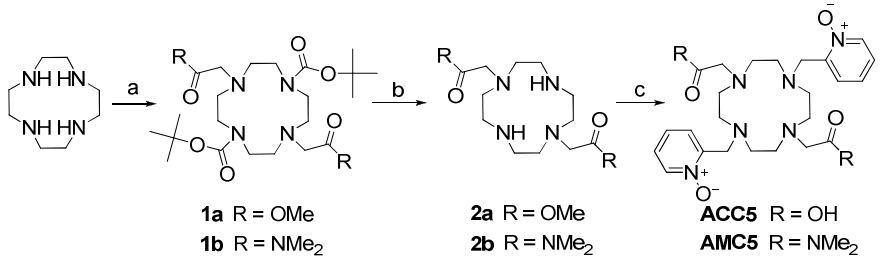

Scheme 1. Synthesis of AMC5. (a) i) BocOSu, $CHCl_3$, RT, 1 day; ii) methyl bromoacetate or 2-chloro-*N*,*N*-dimathylacetamide, K_2CO_3, MeCN, RT, 16 h; (b) TFA, CH_2Cl_2, RT, 4 h; (c) K_2CO_3, 2-(chloromethyl)pyridine-*N*-oxide, MeCN, 80 ^{o}C, 12 h.

The electron donating (OMe) and withdrawing (Cl) analogs of **CLaNP-5** were synthesized as depicted in Scheme 2. Compound **3** was obtained by replacing the nitro group of a commercially available compound, and then reacting it with acetic anhydride to yield the rearranged product **4**. The treatment of **4** with NaOH resulted in hydroxyl **5**. The hydroxyl **7** was also prepared following a published method.[183] Using *m*CPBA, **5** and **7** were converted to *N*-oxides **8a** and **8b**. Treatment of **8a** and **8b** with thionyl chloride gave chloro functionalized compounds, which were directly alkylated with **2a** and **2b**, yielding the precursors of **CLaNP-5** derivatives and **AMC5** analogs, respectively. Removal of the methyl ester of the crude alkylated compounds and coupling with aminoethyl-MTS gave the **CLaNP-5** derivatives.

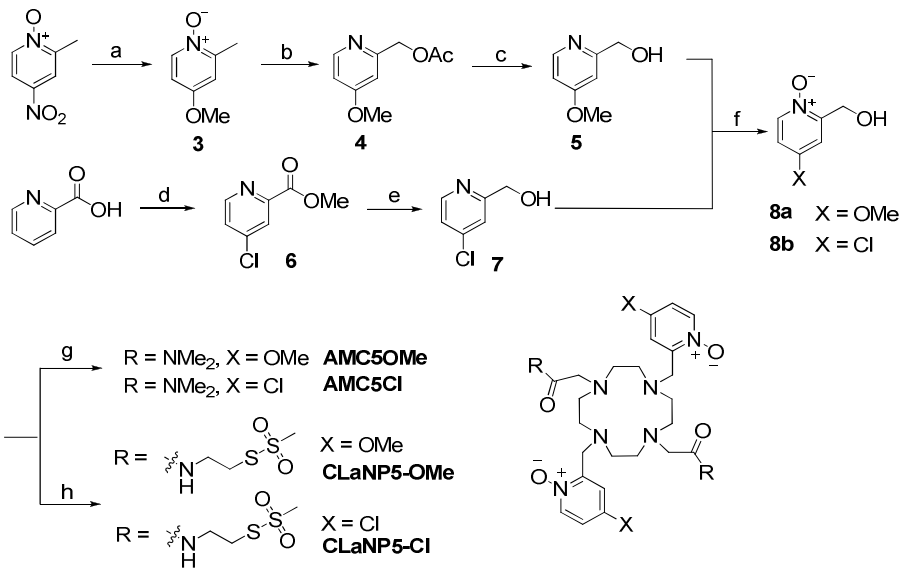

Scheme 2. Synthesis of AMC5OMe, AMC5Cl, CLaNP-5-OMe, and CLaNP-5-Cl. (a) MeOH, K_2CO_3, 70 ^oC, 14 h; (b) Ac_2O, 100 ^oC, 4 h; (c) NaOH, MeOH; (d) i) $SOCl_2$, H_2O, reflux, 3 days; ii) MeOH, toluene, 0 ^oC; (e) $NaBH_4$, MeOH/THF, 0 ^oC; (f) *m*CPBA, $CHCl_3$; (g) i) $SOCl_2$, CH_2Cl_2, RT, 4 h; ii) **2b**, K_2CO_3, MeCN, 50 ^oC; (h) i) $SOCl_2$, CH_2Cl_2, RT, 4 h; ii) **2a**, K_2CO_3, MeCN, 50 ^oC; (iii) NaOH, 1,4-dioxane, RT, 4 h; iv) NHS, EDC, DMF, aminoethyl-MTS, RT, 16 h.

The ^1H NMR spectra of the **AMC5**-series complexes with Eu^{3+} and Yb^{3+} are shown in Figure 1. The assignments of the proton signals were based on 2D EXSY spectra, which give cross-peaks between exchange pairs, and 2D homonuclear COSY experiments, which give strong cross-peaks between the geminal CH_2 protons

and the vicinal protons of the cyclen ring. The most shifted axial cyclen ring proton resonances of all of the Eu^{3+}-complexes were near 20-30 ppm, typical of SA structures,[184] indicating that there is only one enantiomer pair in solution. Moreover, the proton resonances differ between the samples with the different substituents for both lanthanoid complexes, indicating that the magnetic susceptibility is affected by the substituents, although not to a large extend. The lanthanoid induced shift (LIS) is the sum of three contributions: diamagnetic, contact, and pseudocontact shifts (eq 1).

$$\delta_{LIC} = \delta_{dia} + \delta_{con} + \delta_{pcs} \quad \text{(eq 1)}$$

The diamagnetic shift is usually caused by conformational changes, inductive effects, and electric field effects and its value are usually determined using diamagnetic lanthanoid ions (La^{3+}, Lu^{3+}), because that they provide isostructural complexes for the early and the late lanthanoid of the series, respectively. Contact shifts (CS) are through-bond interactions of the unpaired 4f electron spin with the coordinated nucleus, and they decrease rapidly as the number of bonds between the lanthanoid and observed nucleus increases. The pseudocontact shift (PCS) originates from a through-space dipolar interaction between the unpaired electron and observed nucleus. PCS is relevant for protein-protein and protein-ligand interaction. CS is not because the nuclei are too far away or even not bonded in such systems. In the case of Yb^{3+}, the contact shift is usually negligible because it has greatest charge density in the paramagnetic lanthanoid series. As a result, the LIS of Yb^{3+} is dominated by PCSs. As shown in Figure 1, the proton resonances of Yb^{3+} complexes were shifted by changing functional groups, suggesting that the magnetic susceptibilities are different.

To demonstrate the feasibility of our hypothesis, **CLaNP-5-OMe** as well as **CLaNP-5** coordinated to diamagnetic Lu^{3+} and paramagnetic Yb^{3+} were attached to a model protein, ubiquitin (Ub) A28C/D32C and the [^{15}N,^{1}H]-HSQC spectra of labeled proteins are shown in Figure 2. Surprisingly, two sets of PCSs were observed in the case of **CLaNP-5-OMe**, but a single set for **CLaNP-5**. One of these two sets of PCSs was similar to the one of **CLaNP-5** and most of the paramagnetic peaks were merged to “CLaNP5-like” peaks when the temperature was increased. Some resonances showed PCSs of the opposite sign compared to the shift observed with “CLaNP5-like”. Those amide resonances with different sign are located in the same area of protein, as showed in Figure 3. This is indicative of the fact that these two sets of PCSs had differently orientated magnetic susceptibility tensors, the

"CLaNP5-like" state and the "additional" state. The Δχ-tensors and metal positions of **CLaNP-5** and the two states of **CLaNP-5-OMe** were calculated using NUMBAT[168]. The axial ($\Delta\chi_{ax}$) and rhombic ($\Delta\chi_{rh}$) components are reported in Table 1 and the back-calculated PCSs are plotted versus the observed ones in Figure 4. The $\Delta\chi_{ax}$ and $\Delta\chi_{rh}$ of **CLaNP-5-OMe** are similar to those of **CLaNP-5**. The metal positions of the "additional" state and "CLaNP5-like" state based on calculated Δχ-tensors are slightly different (2.3 Å) and Δχ-tensors show a 40^{o} difference in β angle and 30^{o} in γ Euler angles (Table 1). In the case of **CLaNP-7**, a histidine sits close to the attachment site and forms a hydrogen bond with a proposed ninth coordinating ligand, namely water. As a result, the symmetry of probe was broken, yielding two sets of PCSs (Chapter 2). Here, the attachment site is located on an α-helix and a glutamine, Gln31, is close to it. So, in analogy with **CLaNP-7**, the side-chain amide could form a hydrogen bond with the methoxyl oxygen atom of **CLaNP-5-OMe**, twisting the probe and yielding "additional" state. However, in a model of the probe the distance between the side-chain amide proton of Gln31 and the oxygen atom of methoxyl is too long to form a proper hydrogen bond (Figure 5A).

It is worth noting that the amide resonance of residue Glu34, which is close to that attachment site, shows a small shoulder in the HSQC spectrum of Lu-**CLaNP-5** and these peaks become two clear peaks in the case of Lu-**CLaNP-5-OMe** tagged protein. This suggests also in the **CLaNP-5** case there is a minor second state and that in the methoxyl functionalized **CLaNP-5** the population of this state is enhanced to give the "additional" state. DOTA-based lanthanoid complexes such as Eu-**CLaNP-5** are known to undergo enantiomerization with an exchange rate of 200 s^{-1} at 298 K.[111] The ^{1}H NMR spectrum of Yb-**CLaNP-5-OMe** complex shows a single enantiomeric pair in solution (Figure 6). This symmetry is broken when the probe is bound to a chiral protein, resulting in a pair of diastereoisomers. However, the paramagnetic probe may still present a single set of PCSs if both diastereoisomers are similar enough to have identical Δχ-tensors or if one of the diastereoisomers is much more stable than the other. The former seems to be usually the case for **CLaNP-5**. If the diastereoisomers are sufficiently different or if the disulphide bridges can assume two conformations[185], more than a single set of peaks may result. In the present case, the attachment site A28C/D32C is surrounded by several amino acids with long side-chains (Figure 5B), which may interact sterically with the probe

and more strongly with the methoxyl group, yielding two clear sets of PCSs, by either of these mechanisms.

Table 1.PCSs-based Δχ-tensors of Ub A28C/D32C tagged with Yb-CLaNP-5[11] and Yb-CLaNP-5-OMe.

	CLaNP5	CLaNP5-OMe (CLaNP5-like state)	CLaNP5-OMe (additional state)
$\Delta\chi_{ax}$[a]	9.2±0.5	8.0±0.5	9.5±0.6
$\Delta\chi_{rh}$[a]	2.4±0.7	2.7±0.6	3.3±0.5
α	142±4	139±4	147±3
β	87±2	90±2	54±2
γ	91±8	100±8	71±7
Restraints	45	38	33
Q	0.01	0.02	0.01

[a] The unit of axial and rhombic components ($\Delta\chi_{ax}$ and $\Delta\chi_{rh}$) is 10^{-32} m^3.

Conclusion

To develop an alternative method for getting multiple data restraints from a single mutant site, two **CLaNP-5** derivatives as well as a model system were synthesized. The ^{1}H NMR spectra showed that the paramagnetic shift was affected in the derivatives and all presented a single enantiomeric pair in solution. However, the $\Delta\chi_{ax}$ and $\Delta\chi_{rh}$ based on protein data show that **CLaNP-5-OMe** and **CLaNP-5** have similar magnetic susceptibility tensors. It is concluded that remote changes in the coordination system yield changes in the Δχ-tensor that are too small to be of practical use. The functional group does affect the physical behavior of the probe after attachment. The HSQC spectra of **CLaNP-5-OMe** tagged protein presented two sets of PCSs, but a single set for **CLaNP-5**. This could be explained by interactions of the probe with the surrounding amino acids, because of the increased bulkiness of the **CLaNP-5-OMe**.

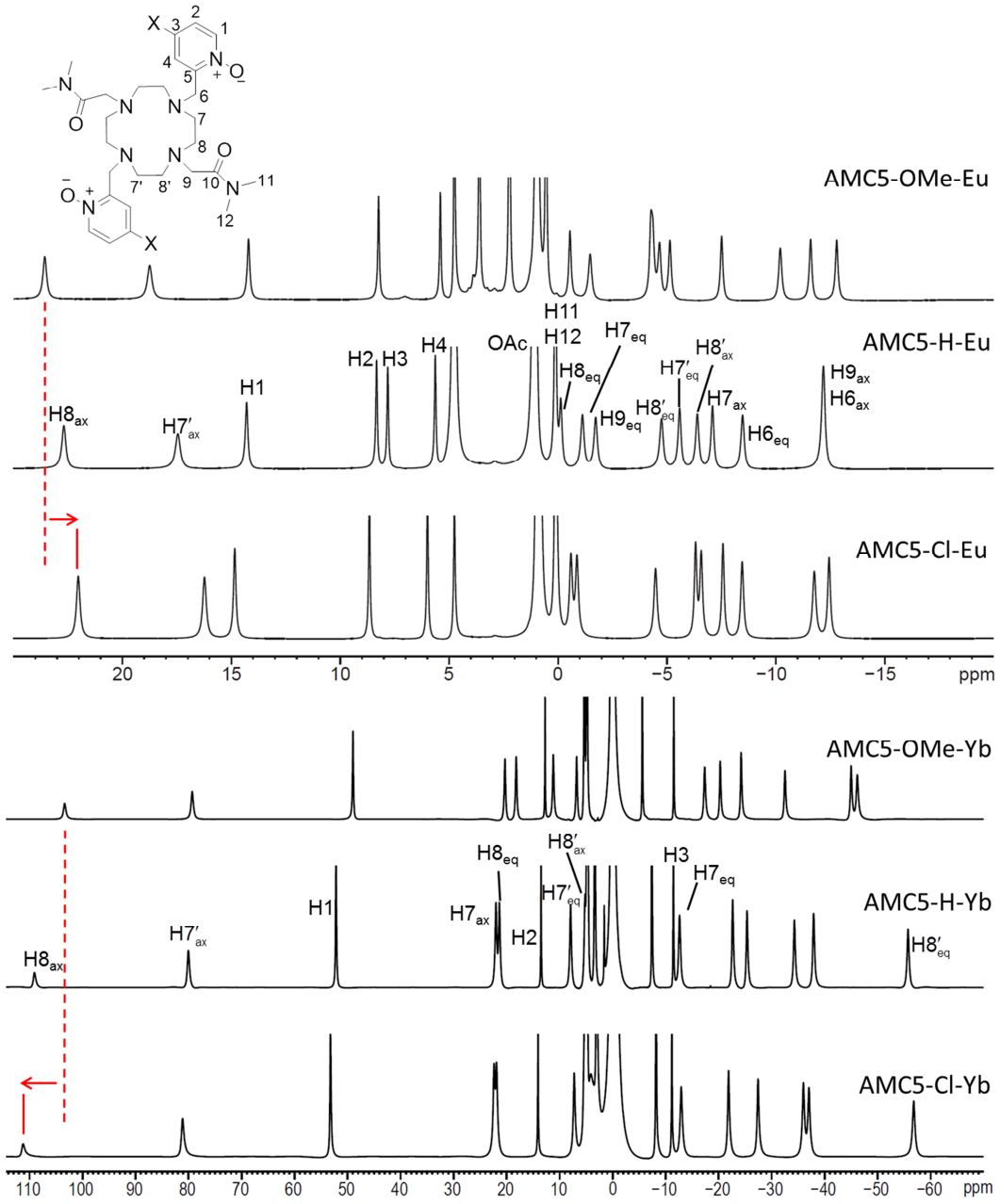

Figure 1. The ^{1}H NMR spectra of Yb^{3+} and Eu^{3+} complexes with AMC5-series. Proton assignments of AMC5-Eu are indicated by corresponding numbers on the structure. The red dashed and red solid lines indicate the positions of the axial ring proton of AMC5-OMe and AMC5-Cl complex resonances, respectively.

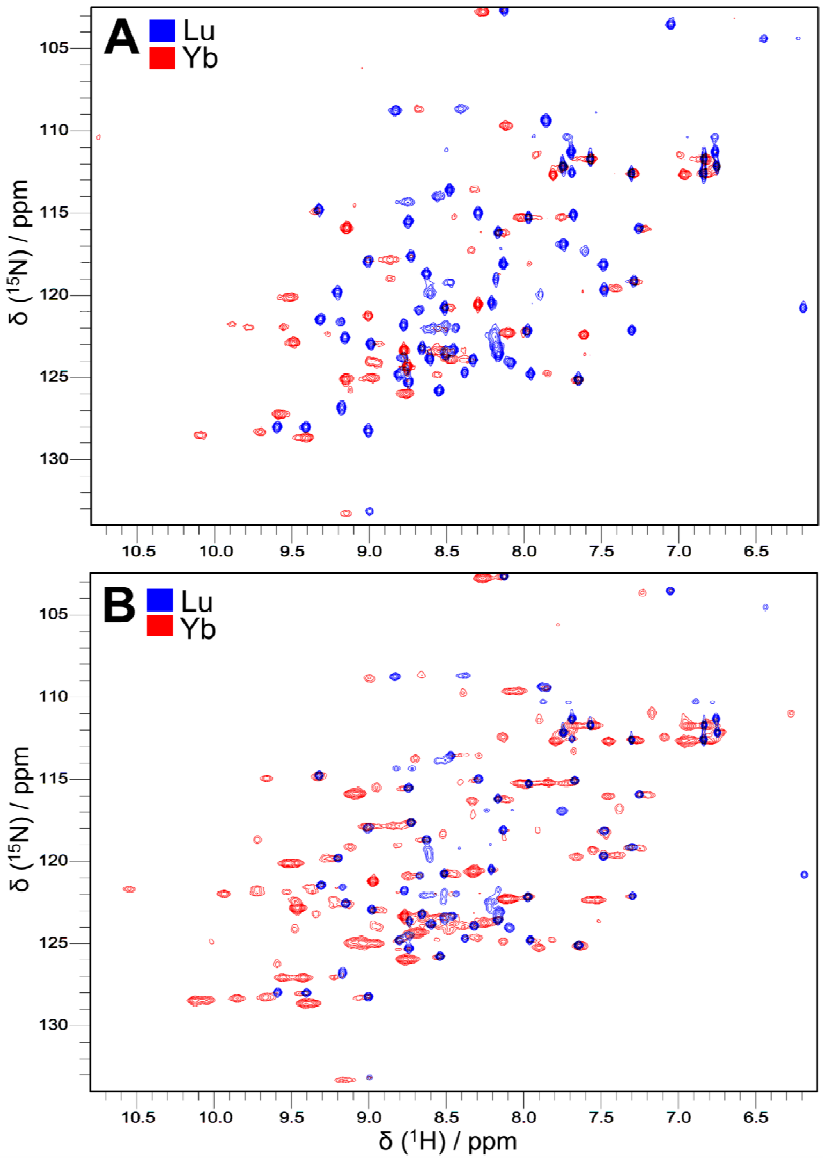

Figure 2. Overlay of [^{15}N, ^{1}H]-HSQC spectra of Ub A28C/D32C attached to CLaNP-5 (A) and CLaNP-5-OMe (B) with diamagnetic Lu^{3+} (blue) and paramagnetic Yb^{3+} (red) at 296 K. Several PCSs are indicated with solid lines.

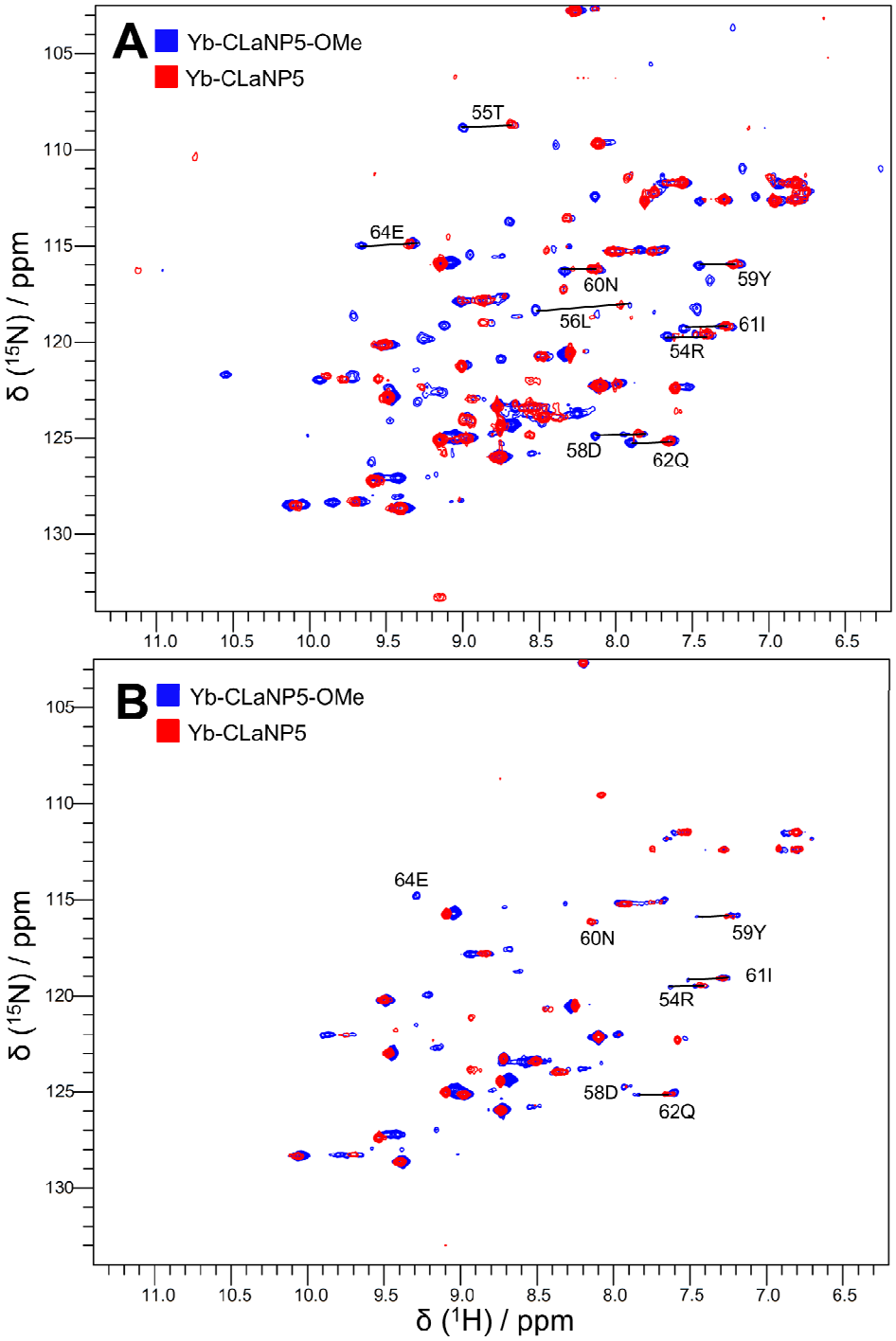

Figure 3. Overlay of [^{15}N, ^{1}H]-HSQC spectra of Ub A28C/D32C attached to Yb-CLaNP5-OMe (blue) and Yb-CLaNP-5 (red) at 296 K (A) and 306 K (B). The assignment of amide proton resonances is indicated in solid line.

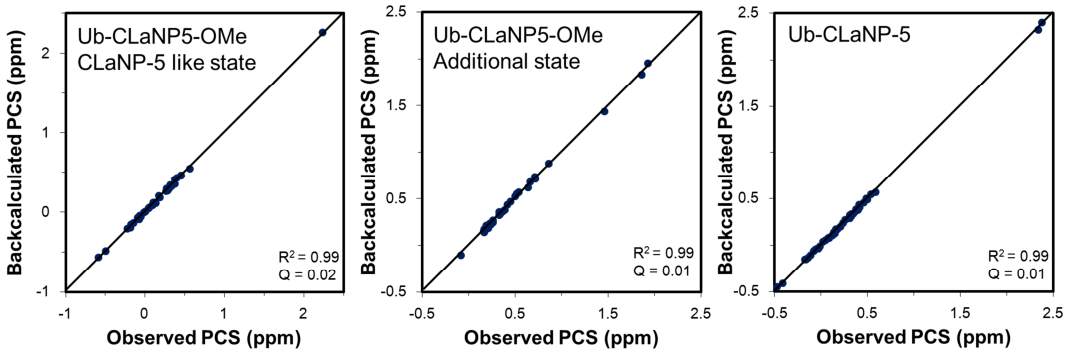

Figure 4. Experimentally observed amide proton PCSs of Ub A28C/D32C Yb-CLaNP-5-OMe and Yb-CLaNP-5 plotted against the back-calculated PCSs. The solid lines represent the perfect correlation (y = x).

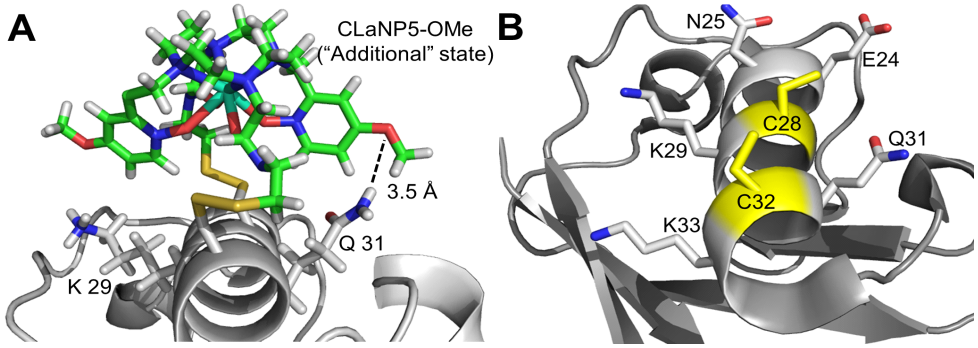

Figure 5. Structure of Ub A28C/D32C attachment site (PDB entry 1D3Z[186]). The Cys residues at positions 56 and 58 were modeled. (A) Model of CLaNP-5-OMe attached to Ub A28C/D32C. The position of the Yb^{3+} (cyanine) is derived from a fit to the PCS data. The distance between the side-chain amide proton of Q 31 and the methoxyl oxygen atom is 3.5 Å. (B) The surrounding amino acids with long side-chains are shown. The protein main chain is shown in grey. The Ub (A28C/D32C) and the N 25, E 24, K 29, Q 31, and K 33 side-chains are shown in CPK colors. The carbon atoms from CLaNP-5-OMe are shown in green, nitrogen atoms in blue, oxygen atoms in red and sulfur atoms in yellow.

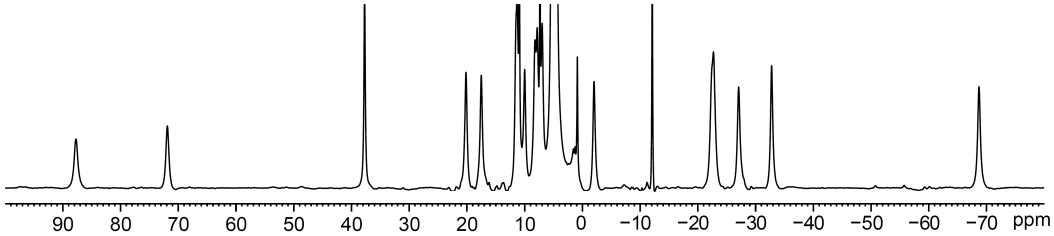

Figure 6. ^{1}H NMR spectra of Yb-CLaNP-5-OMe complex.

Materials and Methods

General

Compound **1a**[42], **1b**[42], **3**[187], **4**[188], **5**[188], **6**[183], and **7**[183] were prepared according to literature procedures and all other chemicals were used as purchased without further purification. TLC-analysis was conducted on DC-alufolien (Merck, Kieselgel60, F254) with detection by UV-absorption (254 nm). Flash chromatography was performed on Screening Devices silica gel 60 (0.04 - 0.06 mm). A Biocad Vision HPLC (PerSeptive Biosystems, inc.) and an Akta Basic FPLC (GE Healthcare Inc.) were used for purifications. Analytical, semipreparative, and preparative reversed phase C18 columns were obtained from Phenomenex (Torrance, CA). Superdex 75 was obtained from GE Healthcare. NMR spectra were recorded on a Bruker AV-400 (400/100 MHz) and Bruker Avance-III 600 (600/150 MHz) spectrometer. A LCQ LCMS system and a Finnigan LTQ Orbitrap system were used for HRMS and protein conjugation analysis. FTIR was performed on a Perkin-Elmer (Shelton, CT) Paragon 1000 FTIR spectrometer. Melting points were obtained using a SMP3 scientific melting apparatus (Stuart, Bibby Sterlin Ltd.)

The synthesis of protective cyclen (1a, 1b)

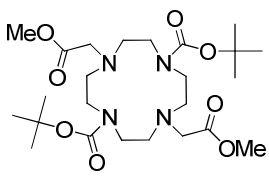

1a and **1b** were prepared according to literature procedures.[42] **1a**: ^{1}H NMR (400 MHz $CDCl_3$): δ = 1.27 (s, 18H), 2.69 (br, 8H), 3.21 (br, 8H), 3.28 (s, 4H), 3.51 (s, 6H). ^{13}C NMR (100 MHz $CDCl_3$): δ = 28.14, 46.21, 50.98, 54.36, 54.54, 79.05, 155.51, 171.39. HR-MS: m/z 517.3225 $[M+H]^+$, calcd $[C_{24}H_{45}N_4O_8]$ 517.3232.

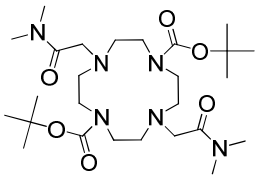

1b: ^{1}H NMR (400 MHz $CDCl_3$): δ = 1.36 (s, 18H), 2.79 (br, 8H), 2.84 (s, 6H), 2.96 (s, 6H), 3.37 (br, 12H) ^{13}C NMR (100 MHz $CDCl_3$): δ = 28.5, 35.4, 36.9, 46.3, 54.5, 56.7, 79.4, 155.9, 170.4. HR-MS: m/z 543.3857 $[M+H]^+$, calcd $[C_{26}H_{51}N_6O_6]$ 543.3864.

ACC5

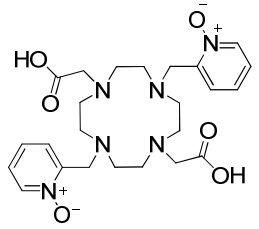

Compound **1a** (273 mg, 0.53 mmol) was dissolved in a 1.5 mL TFA/CH_2Cl_2 (v/v, 3/1) solution mixture and the reaction was stirred at RT for 4 h. After removal the reaction solvent, the residue was co-evaporated with toluene twice and re-dissolved in 5 mL MeCN. 2-(chloromethyl)pyridine-*N*-oxide (167 mg, 1.16 mmol) and K_2CO_3 (167 mg, 1.2 mmol) were added into the solution mixture and it was stirred at 80 ^{o}C for 16 h. The excess K_2CO_3 was filtered off and the filtrate was concentrated *in vacuo*. The concentrated residue was dissolved in a solution mixture which contains 1,4-dioxane (final concentration was 15 mM) and 3 M NaOH (final concentration was 0.4 M) and was stirred at RT for 4 h. Neutralizing and removing the solvent, the crud compound was purified by HPLC (0.1% TFA and a 5-20% acetonitrile gradient on C18 preparative column) to give **ACC5** (160 mg, 60%). HR-MS m/z: 503.2610 $[M+H]^+$, calcd $[C_{24}H_{35}N_6O_6]$: 503.2613. The NMR data agree with literature reported.[11]

AMC5

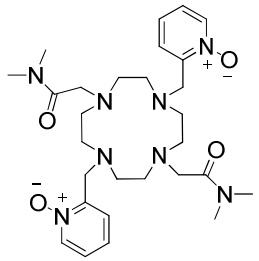

Compound AMC5 was prepared using the same protocol with ACC5 and purified by HPLC (0.1% TFA and a 5-20% acetonitrile gradient on C18 preparative column) in 9% yield. ^{1}H NMR (600 MHz, D_2O, 323 K): δ = 8.37 (d, 2H, *J* = 6.6 Hz), 7.87 (d, 2H, *J* = 7.8 Hz), 7.70 (t, 2H, *J* = 7.2Hz), 7.59 (t, 2H, *J* = 6.9 Hz), 4.19 (s, 4H), 4.07 (s, 4H), 3.56 (br, 8H), 3.11-3.06 (br, 8H), 2.91 (s, 6H), 2.87 (s, 6H). ^{13}C NMR (150 MHz, D_2O, 323 K): δ = 165.6, 146.4, 141.1, 131.9, 130.2, 127.8, 54.9, 52.2, 51.7, 49.1, 36.6, 36.4. HR-MS m/z: 557.3559 $[M+H]^+$, calcd $[C_{28}H_{45}N_8O_4]$: 557.3558.

(4-methoxypyridin-2-yl)methanol-*N*-oxide (8a)

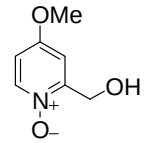

To a solution of **6** (139 mg, 1 mmol) in 5 mL $CHCl_3$ *m*CPBA (295 mg, 1.2 mmol) was added. The reaction was stirred at RT for 10 h and was directly concentrated *in vacuo* without extraction. Using silica column chromatography purified the crude residues yielding **11a** (148 mg, 96 %) as a white solid. R_f = 0.06 (10% MeOH in ethyl acetate). m.p. = 130 ^oC. ^1H NMR (400 MHz, $CDCl_3$): δ = 8.22 (d, 1H, *J* = 6.8 Hz), 7.78 (d, 1H, *J* = 2.4 Hz), 7.65 (dd, 1H, *J* = 6.8, 2.4 Hz), 2.49 (s, 3H), 1.56 (s, 9H). ^{13}C NMR (100 MHz, $CDCl_3$): δ = 162.4, 148.6, 138.9, 127.6, 126.1, 123.2, 82.1, 27.7, 17.4. FTIR: 3059.1, 2806.4, 1625.9, 1469.7, 1431.2, 1201.6, 1029.9, 736.8 cm^{-1}. HR-MS m/z: 156.0654 $[M+H]^+$, calcd $[C_7H_{10}NO_3]$: 156.0655.

(4-chloropyridin-2-yl)methanol-*N*-oxide (8b)

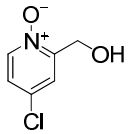

Compound **7** (500 mg, 3.5 mmol) and *m*CPBA (939 mg, 3.8 mmol) were dissolved in 25 mL $CHCl_3$ and the reaction mixture was stirred at RT. However, the starting material was hardly converted to desired product. After stirring for 16 h, the reaction mixture was concentrated *in vacuo* and purified by silica column chromatography. The title compound was obtained in 30% yield. R_f = 0.3 (10% methanol in ethyl acetate). Compound decomposed over 172 ^oC. ^1H NMR (400 MHz, d^4-MeOD): δ = 8.27 (d, 1H, *J* = 6.8 Hz), 7.71 (d, 1H, *J* = 2.8 Hz), 7.5 (dd, 1H, *J* = 6.8 and 2.8 Hz), 4.76 (s, 2H). ^{13}C NMR (100 MHz, d^4-MeOD): δ = 155.3, 141.4, 136.7, 125.9, 124.7, 59.4. FTIR: 3132.4, 3101.5 3072.6, 3028.2, 2918.3, 1850.8, 1606.7, 1423.4, 1211.3, 1055.0, 862.2 cm^{-1}. HR-MS m/z: 160.0158 $[M+H]^+$, calcd $[C_6H_7ClNO_2]$: 160.0159.

AMC5OMe

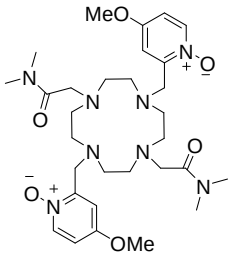

To a solution of **8a** (271 mg, 1.75 mmol) in 10 mL dry CH_2Cl_2 thionyl chloride (229 mg, 1.92 mmol) was slowly added at 0 ^oC with continuous stirring for 2 h. Few drops of MeOH were added to quench the excess thionyl chloride and the reaction solvent was dry *in vacuo*. The crude precursor without any purification was redissolved in a 10 mL MeCN solution containing K_2CO_3 (241 mg, 1.75 mmol) and **2b** (239 mg, 0.7 mmol) and the reaction was stirred at 50 ^oC for 1 day. After filtration with celite, the filtrate was concentration, diluted with

water and purified by HPLC (0.1% TFA and a 5-20% acetonitrile gradient on C18 preparative column) providing **AMC5OMe** in 10% yield. ^{1}H NMR (600 MHz, D_2O, 323 K): δ = 8.41 (d, 2H, *J* = 7.2 Hz), 7.66 (d, 2H, *J* = 3.6 Hz), 7.26 (dd, 2H, *J* = 7.2 Hz, 3.6 Hz), 4.14 (s, 4H), 4.09 (s, 4H), 4.04 (s, 6H), 3.59 (br, 8H), 3.09 (br, 8H), 2.94 (s, 6H), 2.88 (s, 6H). ^{13}C NMR (150 MHz, D_2O, 323 K): δ = 164.8, 164.6, 148.9, 142.8, 116.2, 113.2, 58.2, 55.4, 52.5, 51.6, 48.7, 36.5, 36.4. HR-MS m/z: 617.3768 $[M+H]^+$, calcd $[C_{30}H_{49}N_8O_6]$: 617.3769.

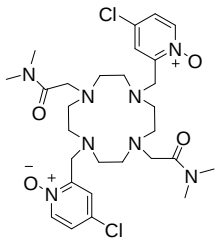

AMC5Cl

The title compound was prepared by following same protocol with **AM5OMe** and purified by HPLC (0.1% TFA and a 5-35% acetonitrile gradient on C30 preparative column) providing **AMC5Cl** in 48% yield. ^{1}H NMR (600 MHz, D_2O, 323 K): δ = 8.33 (d, 2H, *J* = 7.2 Hz), 7.97 (d, 2H, *J* = 3 Hz), 7.61 (dd, 2H, *J* = 7.2 Hz, 3Hz), 4.19 (s, 4H), 4.02 (s, 4H), 3.59 (t, 8H, *J* = 5.4 Hz), 3.06-3.01 (br, 8H), 2.92 (s, 6H), 2.90 (s, 6H). ^{13}C NMR (150 MHz, D_2O, 323 K): δ = 164.6, 148.4, 142.0, 137.8, 129.8, 127.8, 55.1, 52.5, 51.6, 48.8, 36.6, 36.4. HR-MS m/z: 625.2778 $[M+H]^+$, calcd $[C_{28}H_{43}Cl_2N_8O_4]$: 625.2779.

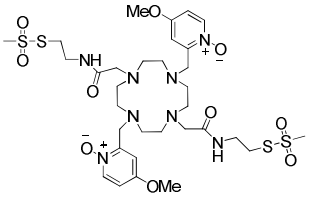

CLaNP-5-OMe

To a solution of **8a** (155 mg, 1 mmol) in 10 mL dry CH_2Cl_2 thionyl chloride (143 mg, 1.2 mmol) was dropwise added at 0 ^{o}C with continuous stirring for 2 h. Few drops of MeOH were added to quench the excess thionyl chloride and the reaction solvent was dry *in vacuo*. The crude precursor without any purification was redissolved in a 10 mL MeCN solution containing K_2CO_3 (207 mg, 1.5 mmol) and **2a** (126 mg, 0.4 mmol) and the reaction was stirred at 50 ^{o}C for 1 day. After filtration with celite, the filtrate was concentration under vacuo and dissolved in 66 mL of 3M NaOH/1,4-dioxane (v:v/3:20) solvent mixture. The crude reaction mixture was stirred for 4 h, neutralized with acid resin, filtered off, and the filtrate was co-evaporated with toluene twice. To a solution of crude residues (44 mg, 0.08 mmol) in 1mL *N*,*N*-dimethylformate NHS (36 mg, 0.3 mmol), EDC (60 mg, 0.3 mmol), and aminoethyl-MTS (46 mg, 0.2 mmol) were added. The reaction was stirred at RT for 16 h and

then diluted with 5 mL water. The crude aqueous solution was purified by HPLC (0.1% TFA and a 0-25% acetonitrile gradient on C18 preparative column) to provide title compound in 15% yield over 4 steps. ^{1}H NMR (600 MHz, D_2O, 323 K): δ = 8.40 (d, 2H, *J* = 7.2 Hz), 7.59 (d, 2H, *J* = 3.6 Hz), 7.26 (dd, 2H, *J* = 7.8 Hz and 3.6 Hz), 4.27 (s, 4H), 4.01 (s, 6H), 3.72 (s, 4H), 3.58 (t, 4H, *J* = 6.6 Hz), 3.48 (s, 8H), 3.44 (s, 6H), 3.43 (t, 4H, *J* = 6 Hz), 3.19 (br, 8H). ^{13}C NMR (150 MHz, D_2O, 323 K): δ = 146.1, 142.5, 116.4, 113.5, 58.0, 55.5, 53.0, 51.5, 50.4, 49.9, 39.6, 36.1. HR-MS m/z: 837.2762 $[M+H]^+$, calcd $[C_{32}H_{53}N_8O_{10}S_4]$: 837.2762.

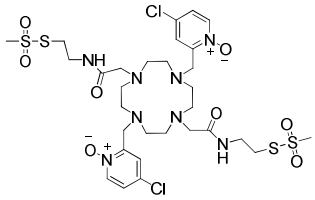

CLaNP-5-Cl

The title compound was prepared by following the same protocol with **CLaNP-5-OMe** and purified by HPLC (0.1% TFA and a 0-25% acetonitrile gradient on C18 preparative column) providing **CLaNP-5-Cl** in 20% yield. ^{1}H NMR (600 MHz, D_2O, 323 K): δ = 8.38 (d, 2H, *J* = 6.6 Hz), 7.99 (d, 2H, *J* = 2.4 Hz), 7.67 (dd, 2H, *J* = 6.6 and 3 Hz), 4.19 (s, 4H), 3.87 (s, 4H), 3.60 (t, 4H, *J* = 6 Hz), 3.54 (s, 8H), 3.45 (s, 6H), 3.35 (t, 4H, *J* = 6 Hz), 3.17 (br, 8H). ^{13}C NMR (150 MHz, D_2O, 323 K): δ = 146.6, 142.0, 137.5, 129.9, 128.1, 55.4, 52.3, 51.8, 50.5, 49.4, 39.6, 36.1. HR-MS m/z: 845.1774 $[M+H]^+$, calcd $[C_{30}H_{47}Cl_2N_8O_8S_4]$: 845.1771.

Preparation of the lanthanoid complexes

To a solution of the **AMC5** derivatives (6 mg ~ 10 mg) in 100 μL D_2O was added 1.1 equiv of $Ln(OAc)_3$. The solution mixture was stirred at RT for 12 h and monitored by LC/MS spectroscopy. When the free **AMC5** derivatives were completely converted to lanthanoid complexes, the solution mixture was diluted with 400 μL D_2O and the pD value was adjusted until 7 by using NaOD. The complexes without further purification were directly used for NMR experiments. The ^{1}H, 2D EXSY and COSY spectra were recorded on a Bruker Avance III 600 MHz spectrometer at 298 K.

Paramagnetic Probe Attachment

The lanthanoid complexes of **CLaNP-5** and **CLaNP-5-OMe** and attachment experiments were prepared according to reported protocol.[11,42] The probe attached

Ub A28C/D32C sample was concentrated to 500 μL and purified over a Superdex 75 gel filtration column. The yield of labeling, estimated from the intensity of diamagnetic peaks in the [^{15}N, ^{1}H]-HSQC spectra of samples with paramagnetic tags, was more than 90%. The mass of the resulting ^{15}N-Ub Yb-**CLaNP5-OMe** (9534 ± 1 Da) agreed with the expected mass of 9535 Da, assuming 95% ^{15}N enrichment. The Ub A28C/D32C protein expression and purification were kindly performed by Carlos Castaneda (University of Maryland). The NMR samples of Ub Ln-CLaNP5 and Ub Ln-CLaNP5-OMe (100-200 μM) were prepared in 20 mM HEPES, 100 mM NaCl buffer and pH = 7.2 with 6% (v/v) D_2O. All [^{15}N, ^{1}H]-HSQC were recorded on a Bruker Avance III 600 MHz spectrometer and data were processed with NMRPipe.